Rapid generation of highly uniform droplets using asymmetric microchannels fabricated on a single crystal silicon plate

Goran T. Vladisavljević[1†], Isao Kobayashi[2], Mitsutoshi Nakajima[2]

[1]*Chemical Engineering Department, Loughborough University, Loughborough, Leicestershire LE11 3TU UK*

[2]*National Food Research Institute, National Agriculture and Food Research Organization, Kannondai 2-1-12, Tsukuba, Ibaraki, Japan 305-8642.* [†]Corresponding author, e-mail: G.Vladisavljevic@lboro.ac.uk

1. Introduction

A microfluidic device can be identified by the fact that it has one or more channels with at least one dimension less than 1 mm. The most common types of microfluidic devices are: (i) soft microfluidic devices fabricated in elastomeric materials such as PDMS by soft lithography [1], (ii) glass devices manufactured in quartz glass or glassy polymers such as PMMA by etching or micromachining [2], and (iii) microchannel (MC) array devices fabricated in silicon by photolithography and wet-etching or deep-reactive ion etching processing [3]. Microfluidic devices can be used for capillary electrophoresis [4], liquid-liquid extraction [5], immunoassays [6], cellomics [7], proteomics [8], DNA analysis [9], blood rheology measurements [10], microreactors [11], droplet formation [2], etc. The soft microfluidic devices such as T-junctions and flow focusing devices are suitable for rapid generation of monodispersed droplets with a coefficient of variation (CV) in a dripping regime of generally less than 3 %. Although the frequency of drop production can be as high as 7000 Hz, the overall productivity in terms of volume flow rate of the disperse phase is very low because the droplets are formed from a single channel. Silicon MC array devices are much more suitable for large-scale applications because the total number of microchannels on a chip can be hundreds of thousands.

The aim of this work was to investigate the generation of uniform droplets at high production rates using novel asymmetric MC array microfabricated on a silicon plate [12]. Monodispersed emulsion droplets are much more favourable both in fundamental studies and practical applications. Emulsion appearance and rheology, stability against Oswald ripening and creaming, and the suitability of droplets as templates to the production of solid micro- and nano-particles are strongly influenced by their particle size distribution.

2. Experimental

The experiments have been carried out using silicon 24 × 24 mm MC plates (EPT Tech, Hitachi, Japan, model WMS1-3) containing 23,348 MCs arranged within a 10 × 10 mm central region. As shown in Fig. 1A, the plate was 500 μm thick, but it was thinned down to thickness 100 μm in the central region. The plates were microfabricated by photolithography and deep reactive ion etching (DRIE). Each MC consists of a circular 10 μm-diameter straight hole with a depth of 70 μm and a 50 × 10 μm microslit with a depth of 30 μm. Before first usage, the plate was subjected to plasma oxidation in a plasma reactor (PR41, Yamato Science Co. Ltd., Tokyo) for a hydrophilic silicon dioxide layer to be formed on the surface. After each experiment the plate was cleaned in an ultrasound water bath (Iuchi, VS-100 III) using a commercial detergent solution and stored in 0.1 M nitric acid solution to maintain its hydrophilic nature. The experiments have been carried out using 2 wt% Tween 20 or 0.01-2 wt% SDS (sodium dodecyl sulphate) dissolved in Milli Q water as a continuous phase. The disperse phase was soybean oil, MCT (middle-chain fatty acid triglyceride) oil or tetradecane with a viscosity at 293 K of 50, 20, and 2.7 mPa·s, respectively. The MC plate was degassed in the continuous phase by ultrasound treatment for 20 min prior to each experiment. The dispersed phase was injected through the channels by a syringe pump (Harvard Apparatus, model 11 Plus or PHD 2000) at different flow rates ranging from 1 to 250 mL/h, which was equivalent to the flux values between 10 and 2,500 L/(m^2h). The droplets were created at the outlet of the slits and swept away from the plate surface by continuous phase passing in cross flow. The continuous phase flow rate ranged from 50 mL/h at the oil flow rate of 1 mL/h to about 10,000 mL/h at the highest oil flow rates. It means that the droplet concentration in the outlet emulsion stream was 2 vol % at the oil flow rate of 1 ml/h.

The droplet generation was observed in real time using a high-speed camera attached to a microscope. The particle size distribution of the resultant emulsion droplets was measured using a commercial light scattering instrument (Beckman Coulter LS 13 320, Miami, FL).

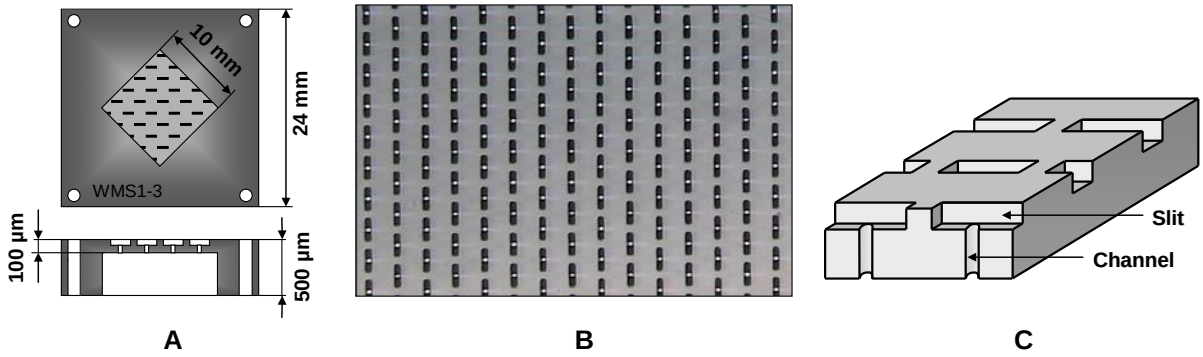

Fig 1A: Schematic drawing of WMS1-3 MC plate (top and cross sectional view); Fig. 1B: Micrograph of the surface of WMS1-3 plate. (The plate was illuminated from the bottom side so the circular channels were visible as bright dots in the centre of each slit); Fig. 1C: Schematic view of the asymmetric structure of MCs.

3. Results and discussion

3.1 Effect of emulsifier content in continuous aqueous phase

The effect of emulsifier (SDS) in the continuous phase was investigated over a wide concentration range between 0.01 and 2 wt% using soybean oil as a dispersed phase. The oil flow rate was kept constant at 1 mL/h, which was equivalent to the oil flux of 10 L/(m^2h) and the continuous phase flow rate was 50 mL/h. As shown in Fig. 2, irrespective of the SDS concentration highly monodispersed emulsion droplets were obtained with a span of particle size distribution typically in the range of 0.210-0.225 [span = $d_{50}/(d_{90}-d_{10})$], although a very low span value of 0.087 was obtained in one experiment, as can be seen in Fig. 4. The highest span value of 0.225 ± 0.007 has been obtained at 0.01 wt% SDS. However, even at this very low SDS concentration of 0.01 wt% which is well below the critical micelle concentration of SDS in pure water of 0.2-0.25 wt%, the generated oil droplets were monodispersed, which could be explained by the presence of surface-active agents in soybean oil, such as free fatty acids (e.g., linoleic acid).

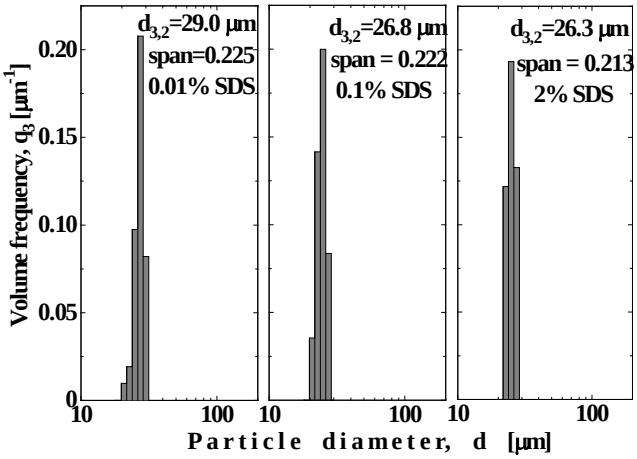

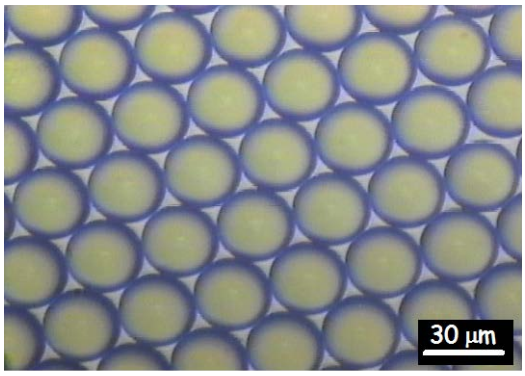

Fig 2 (left): Particle size distribution of the resultant soybean oil droplets at three different concentrations of SDS (J=10 L/(m^2h)). Fig. 3 (right): Micrograph of the emulsion droplets at the SDS concentration of 0.2 wt %.

In the experiments with very low SDS concentration (0.01-0.1 wt%), the following problems have been identified: (i) At the SDS concentration of 0.01 and 0.02 wt.%, the soybean oil droplets were not stable against coalescence during storage at room temperature and (ii) some droplets have been attached to the plate surface after creation due to high interfacial tension force (Fig. 4(b)). It might cause some undesirable steric hindrance effects and may lead to the decrease in droplet size uniformity at the higher oil fluxes. As shown in Fig. 4, over the range of SDS concentration of 0.5-2 wt%, which was above CMC, the mean droplet size was unaffected by the SDS concentration. Over the range of SDS concentration of 0.01-0.1 wt% which is below the CMC, the mean droplet size increased by 8 % as the SDS concentration decreased from 0.01 to 0.1 %, which was a consequence of the increased interfacial tension force and the droplets were detached at larger size. Above the CMC, however, satellite droplets with the diameter of about 1 μm were formed from some of the channels, as shown in Figs. 5(a) and 5(b). In addition to that, direct generation of small droplets was observed from some of the channels in some experimental runs, as shown in Fig. 6(c). We assume that this phenomenon occured when the interior of the channel was partially blocked by small impurities in the aqueous phase. The optimum SDS concentration was in the range of 0.2-0.5 wt%, because droplet coalescence might occur at the SDS contents of less than 0.2 wt% and the satellite droplets may form at the SDS concentrations higher than 0.5 wt%.

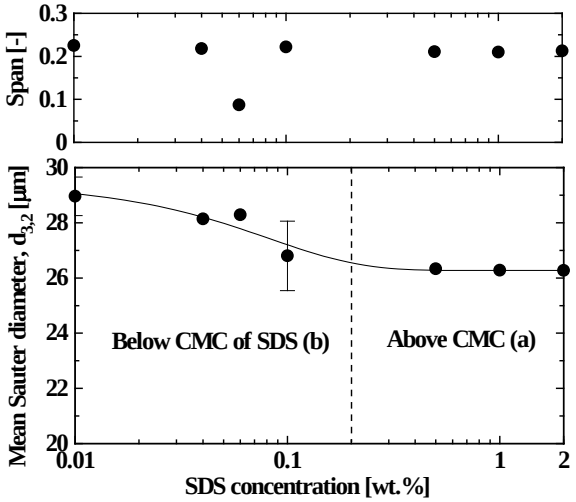

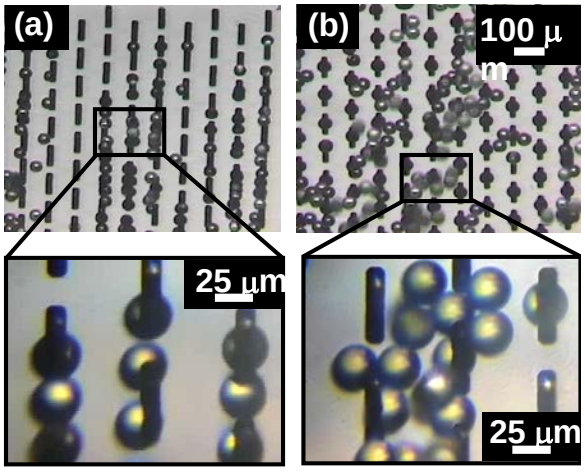

Fig. 4 (left): Effect of SDS concentration in the aqueous phase on the mean size of soybean oil droplets and the span; Fig. 5 (right): Generation of soybean oil droplets at high (a) and low (b) emulsifier content.

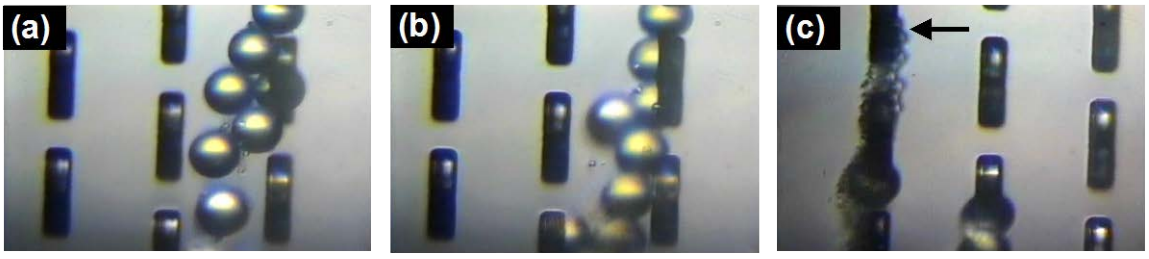

Fig. 6(a) and 6(b): Formation of satellite droplets at 1 wt% SDS; Fig. 6(c): Direct formation of small droplets from a channel clogged by dust particles. The location of this channel is marked by arrow.

3.2 Effect of oil flux

One of the major advantages of asymmetric MC plates is its ability to generate monodispersed droplets at very high frequencies, especially when low- and medium-viscosity oils are used as a disperse phase. Fig. 7 illustrates the oil flux vs. mean particle size for MCT oil, which is a medium-viscosity oil. Up to the flux value

of J=150 $Lm^{-2}h^{-1}$, i.e. within the 'size-stable' zone, the mean droplet size $d_{3,2}$ ranged in a narrow interval from 27.1 to 27.6 μm and was therefore virtually independent on the oil flux and the generated droplets were highly uniform (span = 0.21-0.23). In the range of oil flux between 150 and 600 $Lm^{-2}h^{-1}$ (the 'size-expanding' zone), $d_{3,2}$ increased from 27.6 to 31.2 μm and a span of the particle size distribution was in the range of 0.20-0.25, indicating that the droplets can still be regarded as very uniform. Above the critical flow rate of 600 $Lm^{-2}h^{-1}$ (the 'continuous outflow' zone), the large droplets formed at some channels, as shown in Fig. 8 (b) and a span was in the range of 0.75-0.95, due to the formation of both small and large droplets. In all practical applications, it is critically important to generate monodispersed droplets at reasonable high production rates, therefore the optimum flux for the given MCT oil would be in the range of 200-600 $Lm^{-2}h^{-1}$. Fig. 9 shows a typical particle size distribution of the resultant emulsion droplets for the three regimes depicted in Fig. 7.

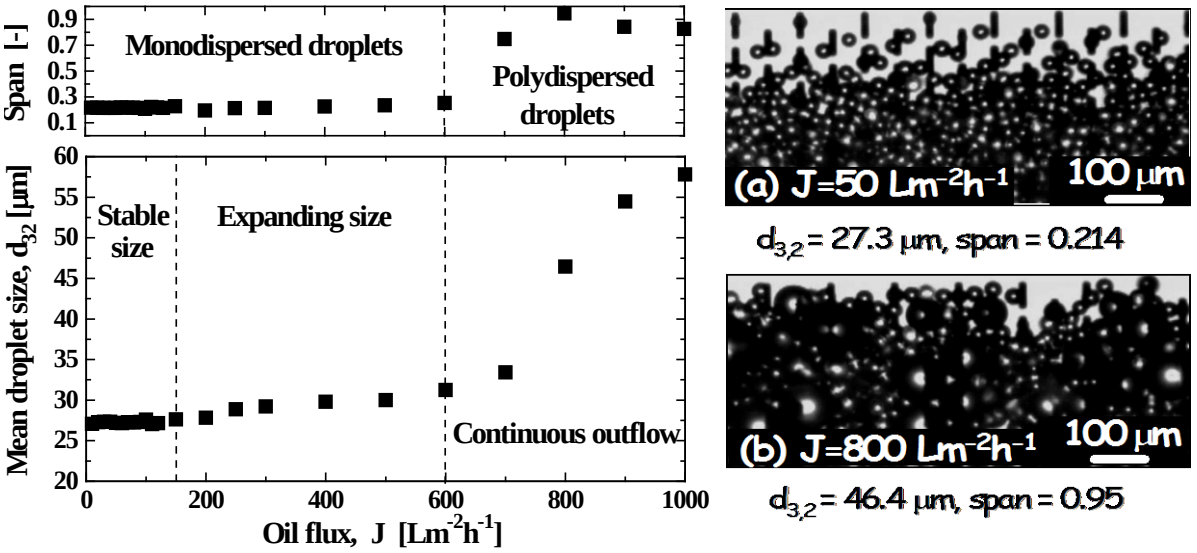

Fig. 7 (left): Effect of oil flux on the mean droplet size and the span of particle size distribution for MCT oil in the presence of 2 wt% Tween 20 in the continuous phase; Fig. 8 (right): Generation of MCT oil droplets below (a) and above (b) the critical oil flux of 600 $Lm^{-2}h^{-1}$.

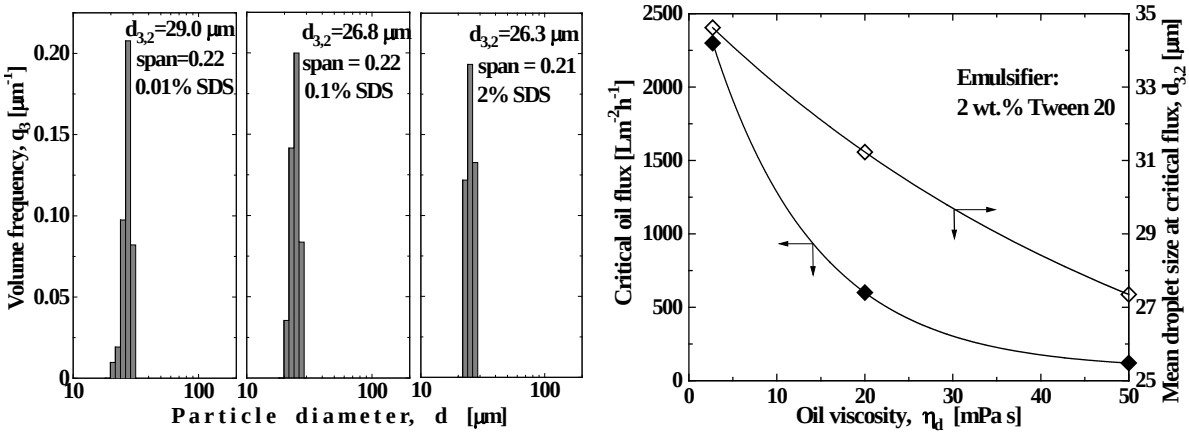

Fig. 9 (left): Typical particle size distribution of MCT oil droplets in size-stable zone (a), size-expanding zone (b) and continuous-outflow zone (c); Fig. 10 (right): Critical oil flux and mean droplet size at the critical oil flux as a function of oil viscosity.

3.3 Effect of oil viscosity

We have found that the critical oil flux increased with decreasing the oil viscosity and was 120 $Lm^{-2}h^{-1}$ for high-viscosity soybean oil and 2300 $Lm^{-2}h^{-1}$ for n-tetradecane, as shown in Fig. 10. It is an exceptionally high critical flux and such a high flux value has not been reported earlier in any MC emulsification work. The critical flux was defined here as a flux value corresponding to the span of particle size distribution of around 0.25. The span values were generally less than 0.25 below the critical flux and larger than 0.25 above the critical flux. The mean particle size at the critical flux significantly decreased as the oil viscosity decreased. The oil viscosity greatly affected the mean drop generation rate from active channels, as shown in Fig. 11. At the same capillary number, the mean droplet generation rate was much higher for n-tetradecane (TD) than for other oils. The maximum droplet generation rate for TD of 233 drops/s in Fig. 11 was observed at the oil flux of 1900 $Lm^{-2}h^{-1}$. In spite of this extremely high flux, the particle size distribution span was just 0.229 ± 0.004, which clearly shows capability of asymmetric MCs to generate monodisperse droplets at very high frequencies.

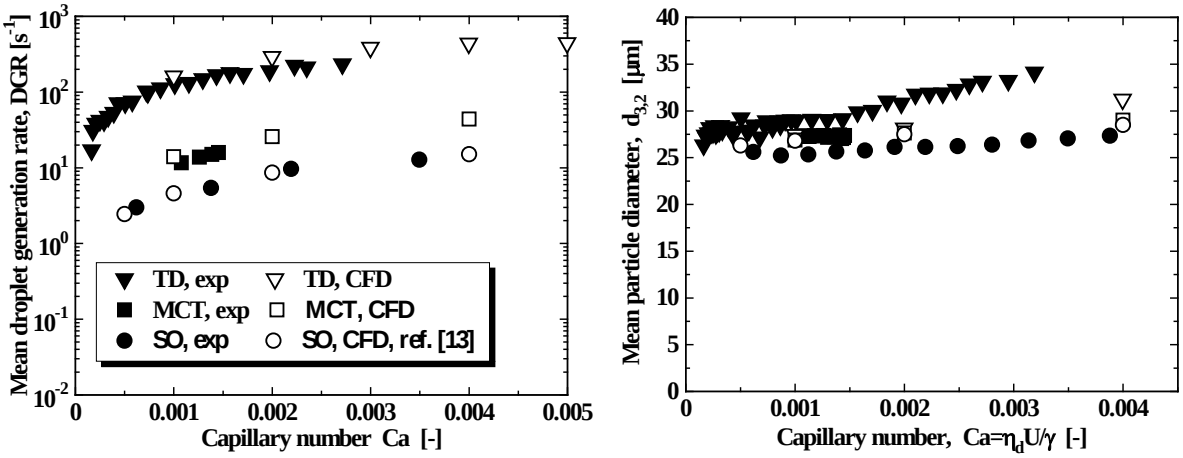

Fig. 11 (left): Mean droplet generation rate from active channels vs. capillary number for n-tetradecane (TD), MCT oil (MCT) and soybean oil (SO) – experimental data and CFD simulation data; Fig. 12 (right): mean particle size vs. capillary number for n-tetradecane, MCT oil, and soybean oil (emulsifier: 2% Tween 20).

The capillary number Ca was calculated here as $U\eta_d/\gamma$, where U is the mean oil velocity in active channels, η_d is the oil viscosity, and γ is the interfacial tension at oil-aqueous phase interface at the moment of detachment. The droplet formation time was very short (less than 10 ms), so that γ was assumed to be equal to the interfacial tension at the interface between pure water and oil, i.e. the mass transfer of emulsifier molecules to the interface was neglected due to short time between the droplet appearance on the plate and detachment. The agreement between the experimental and CFD (Computational Fluid Dynamics) simulation data for the mean droplet generation rate was respectable, especially for soybean oil, as shown in Fig. 11. The agreement between the experimental and simulation data for the mean particle diameter is also satisfactory, except for tetradecane at high capillary numbers, as can be seen from Fig. 12. The mean droplet generation rate k can be calculated from the mass balance equation for oil: $Q_d = JA = k \cdot DGR \cdot N \cdot V_d$, where Q_d is the flow rate of oil through the plate measured by the syringe pump, $A = 1\ cm^2$ is the effective cross-sectional area of MC plate, DGR is the mean droplet generation rate estimated from the video recordings captured by high-speed camera, N = 23,348 is the total number of MCs within the plate, and V_d is the mean droplet volume given by $d_{4,3}{}^3 \cdot \pi/6$. Therefore, the fraction of active channels is given by: $k = 6 \cdot Q_d \cdot A/(d_{4,3}{}^3 \cdot \pi \cdot DGR \cdot N)$. In Fig. 13, the percent of active channels calculated using the given equation is plotted against the oil flux. The percent of active channels increased with increasing the oil flux and oil viscosity. A large difference in the number of active channels at different fluxes is shown in Fig. 14 for the generation of n-tetradecane droplets. At 10 $Lm^{-2}h^{-1}$, the droplets were generated only from =4 % of the channels, whereas at the oil flux of 500 $Lm^{-2}h^{-1}$ more than 40 % of the channels were active. However, for soybean oil at the flux of J = 10 $Lm^{-2}h^{-1}$, about 50 % of the channels were

active, which was more than 10 times higher value than for n-tetradecane at the same flux. It was counterbalanced by the higher droplet generation rate for TD than for soybean oil, as shown in Fig. 11.

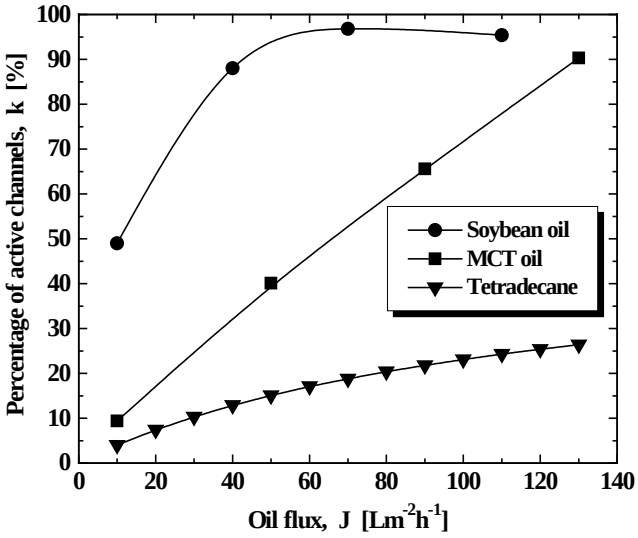

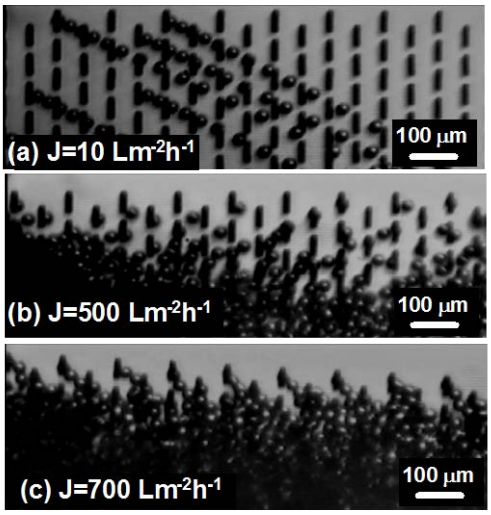

Fig. 13 (left): Effect of oil flux on the percentage of active channels; Fig. 14 (right): Images captured from the video recordings showing generation of tetradecane droplets at different fluxes (emulsifier: 2 wt% Tween 20).

4. Conclusions

Highly monodispersed droplets of soybean oil, MCT (middle-chain fatty acid triglyceride) oil and tetradecane have been generated at high production rates using asymmetric silicon microchannel plates. The critical oil flux for n-tetradecane was 2300 $Lm^{-2}h^{-1}$, which was one of the highest flux values ever reported in MC emulsification. The critical oil flux decreased as the oil viscosity decreased. The mean droplet generation rate increased with decreasing the oil viscosity and was over 250 s^{-1} for tetradecane in the vicinity of critical flux. We demonstrated the ability of asymmetric MC plates to create monodispersed soybean oil droplets at very low emulsifier (SDS) concentration of 0.01 wt%. At too low SDS concentrations, however, droplets tend to attach to the MC plate due to high interfacial tension force, whereas at the SDS concentration of 0.1 wt% or higher they detach from the plate surface as soon as they are formed. In the 'size-stable' zone, the span of the particle size distribution was 0.20-0.22 for both soybean and MCT oil and 0.22-0.26 for n-tetradecane.

5. References

[1] Y. Hia, G. M. Whitesides, *Annu. Rev. Mater. Sci.* 28 (1997) 153.
[2] S. Okushima, T. Nisisako, T. Torii, T. Higuchi, *Langmuir* 20 (9905) 204.
[3] T. Kawakatsu, Y. Kikuchi, M. Nakajima, *J. Am. Oil Chem. Soc.* 74 (1997) 317.
[4] J. Kameoka, H.G. Craighead, H.W. Zhang, J. Henion, *Anal. Chem.* 73 (2001) 1935.
[5] H. Chen, Q. Fang, X.F. Yin, Z.L. Fang, *Lab. Chip* 5 (2005) 719.
[6] A. Hatch, A.E. Kamholz, K.R. Hawkins, M.S. Munson, E.A. Schilling, B.H. Weigl, P. Yager, *Nature Biotechnology* 19 (2001) 461.
[7] H. Andersson, A. van den Berg, *Sensors and Actuators B* 92 (2003) 315.
[8] D. Figeys, D. Pinto, *Electrophoresis* 22 (2001) 208.
[9] M.A. McClain, C.T. Culbertson, S.C. Jacobson, J.M. Ramsey, *Anal. Chem.* 73 (2001) 5334.
[10] Y. Kikuchi, K. Sate, H. Ohki, T. Kaneko, *Microvasc. Res.* 44 (1992) 226.
[11] M. Brivio, R.H. Fokkens, W. Verboom, D.N. Reinhoudt, *Anal. Chem.* 74 (2002) 3972.
[12] I. Kobayashi, S. Mukataka, M. Nakajima, *Langmuir* 21 (2005) 7629.
[13] Kobayashi *et al.*, 38th Autumn Meeting of the Society of Chemical Engineering, Japan, A125 (2006).